P-3

A NEW CLASS OF E-PLANE INTEGRATED MILLIMETER-WAVE FILTERS

Jens Bornemann

Department of Electrical and Computer Engineering
University of Victoria, P.O. Box 1700
Victoria, B.C., Canada V8W 2Y2

ABSTRACT

A new class of E-plane integrated circuit millimeter-wave bandpass filters is introduced which provide high skirt selectivity by comprising inductively coupled stop-band sections. The structure is simple, fully compatible with the E-plane manufacturing process, and does not require fine tuning elements. The design procedure is based on an efficient but rigorous modal S-matrix method including higher-order mode interactions and finite metallization thicknesses. Optimized design data are presented for 33 and 94 GHz in Ka- and W-band, respectively.

I. INTRODUCTION

All-metal insert E-plane integrated circuit filters [1] are well established low-cost, low-loss and mass-producible components in microwave and millimeter-wave technology. Numerical design calculations [2] are in extremely close agreement with measurements (up to 150 GHz) [3], and steps have been taken to improve the passband separation as well as the stopband attenuation [4, 5].

However, the moderate skirt selectivity of these filters compared with dual-mode resonator designs, e.g. [6-8], is still a disadvantage. Since increasing the number of resonators usually leads to higher insertion loss [9], and since metal insert filters are not suitable for dual-mode operation, one way to accomplish improved skirt selectivity is to add stopband circuits capable of providing attenuation peaks in the overall frequency response. This can be achieved by mounting slot- or iris-coupled waveguide resonators on top of the filter housing [10]. A different approach using two-path cutoff waveguide dielectric resonator filters is proposed in [11]. However, none of these structures is suitable for E-plane integrated circuit fabrication.

This paper presents a new class of E-plane metal insert filters (Fig. 1), where attenuation peaks in the bandpass filter response are provided by inductively coupled waveguide resonators rather than by slot-coupled ones. Therefore, the structure is fully compatible with millimeter-wave integrated circuit designs and the low-cost E-plane manufacturing process.

Since the computer-aided design method is based on a rigorous field theory treatment including higher-order mode interactions and the finite thickness of the metal strips, no post-tuning elements, such as screws or sliding shorts, are required.

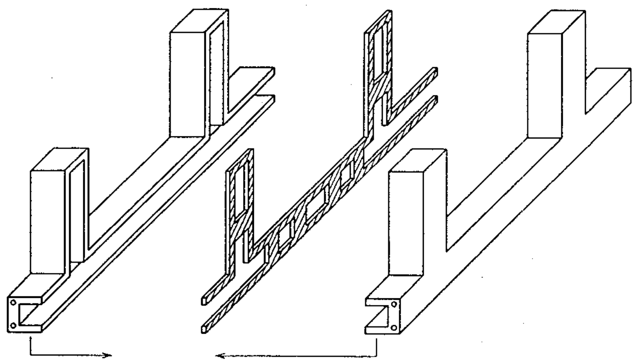

Figure 1. Perspective view of the new E-plane filter.

II. THEORY AND DESIGN

The field theory treatment of the new E-plane filter structure is based on a selected-mode scattering matrix method. Assuming an incident TE_{10} wave, the conventional metal insert filter can be analyzed by a set of longitudinal section TE^{z}_{m0} modes [2, 3], whereas the E-plane waveguide T-junction calculation requires TE^{z}_{1n} modes [12]. This adds up to the five field components of the TE^{z}_{mn} mode spectrum, which sufficiently describes the behavior of the field within the structure as long as b is less than d_3 and d_6 (c.f. Fig. 2b).

CH2725-0/89/0000-0599$01.00 © 1989 IEEE

Therefore, the electromagnetic field in each homogeneous subregion

$$\begin{aligned}\vec{E} &= \nabla \times (A_{hz}\vec{e}_x) \\ \vec{H} &= \frac{j}{w\mu} \nabla \times \nabla \times (A_{hz}\vec{e}_x)\end{aligned} \tag{1}$$

may be expressed in terms of corresponding eigenfunctions. The vector potential function A_{hz} then takes the form

$$\begin{aligned}A_{hz} = \sum_{m=1}^{M} \sum_{n=0}^{N} A_{mn} \sin(k_{xm}x) \frac{\cos(n\pi y/b)}{\sqrt{1+\delta_{on}}} \cdot \\ \cdot [V_{mn} \exp(-jk_{zmn}z) - R_{mn} \exp(+jk_{zmn}z)] \\ \delta_{on} = \text{kronecker delta}\end{aligned} \tag{2}$$

V_{mn} and R_{mn} are the amplitudes of forward and backward traveling waves, respectively, k_{zmn} is the related propagation constant in that subregion, and k_{xm} equals $2m\pi/(a-t)$ in metal insert sections or $(2m-1)\pi/a$ in waveguide sections to account for the $y-z$-symmetry plane at $x = a/2$ (Fig. 2a). A_{mn} is used to normalize the power to $1W$ (propagating mode) or $j1W$ (evanescent mode). Since the waveguide height is kept constant

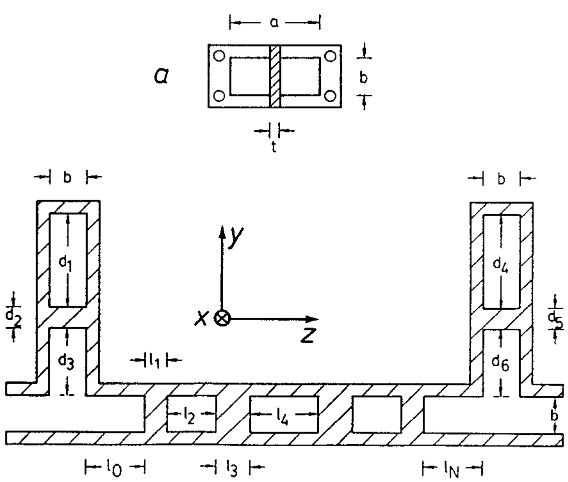

Figure 2. E-plane integrated circuit filter with improved skirt selectivity; a) Metal insert mounted in waveguide housing; b) Sideview.

for both, the metal insert filter section $(l_0 - l_N)$ and the E-plane stubs $(d_1 - d_6)$, eqn. 2 is used to represent the corresponding stub sections by exchanging y and z.

According to Kuehn [13] the waveguide T-junction may be regarded as a resonator area formed by width a, height b and length b. Its vector potential function is a superposition of the eigenfunctions of the three common cross-sections left, right and above the resonator area (c.f. Fig. 2b) [13]. Matching the resonator modes to those of the connected waveguides yields the modal scattering submatrices $\underline{S}_{11}$ to $\underline{S}_{33}$ of the three-port T-junction [12, 13]. With the matrix $\underline{S}_{S11}$ containing the input reflection coefficients for the stub $(d_1 - d_3)$ the overall two-port S-matrix $\underline{S}_G$ of the T-junction including the stub is given by

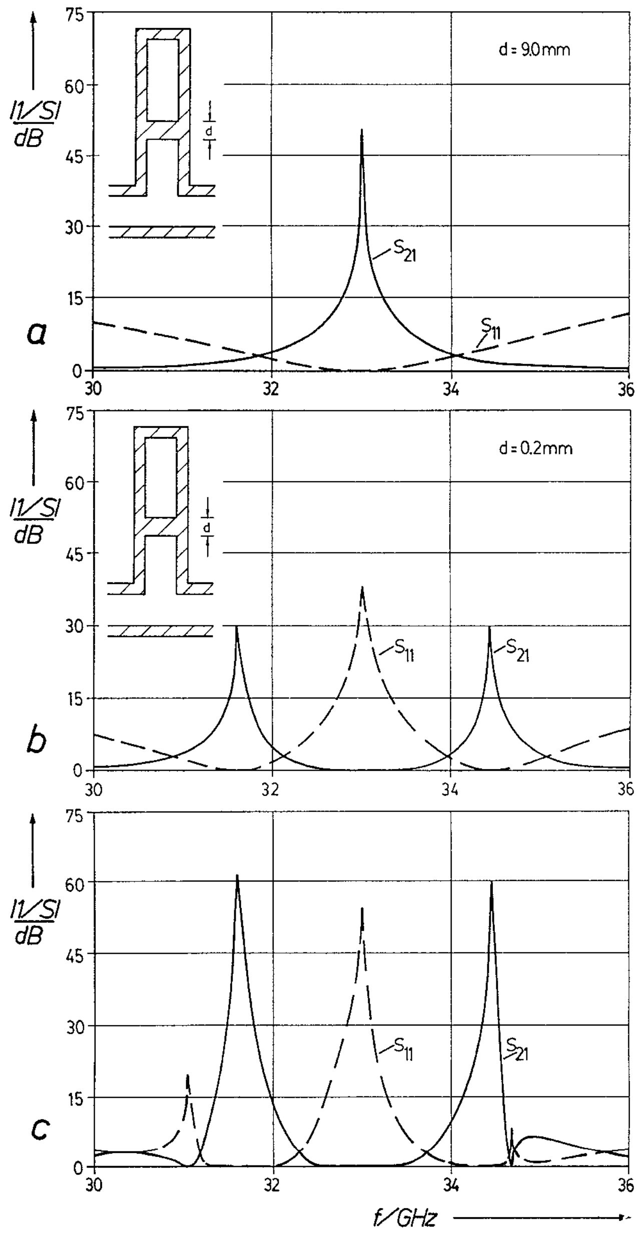

Figure 3. Responses of inductively coupled waveguide stopband circuits: $a = 2b = 7.112$mm, $t = 0.19$mm, $d_1 = 10.951$mm, $d_3 = 7.395$mm; a) $d_2 = 9.0$mm; b) $d_2 = 0.2$mm; c) Two circuits, $l_o + l_N = 18.0$mm.

$$\underline{S}_{G11} = \underline{S}_{G22} = \underline{S}_{11} + \underline{S}_{13}\underline{S}_{S11}[\underline{U} - \underline{S}_{33}\underline{S}_{S11}]^{-1}\underline{S}_{31}$$

$$\underline{S}_{G21} = \underline{S}_{G12} = \underline{S}_{21} + \underline{S}_{23}\underline{S}_{S11}[\underline{U} - \underline{S}_{33}\underline{S}_{S11}]^{-1}\underline{S}_{31} \tag{3}$$

Finally, the overall modal scattering matrix is obtained by cascading the remaining two-port S-matrices [2, 3, 9].

In the computer analysis, only the two general discontinuities (bi-furcation, T-junction) are calculated by up to M=35 and N=25 modes. For all S-matrix combining algorithms, however, only the lowest five to seven types are selected. This considerably speeds up the program and provides data within the plotting accuracy compared with the full-mode analysis. The CPU time for one set of input parameters is about 10 minutes on an enhanced personal computer. The design is carried out by pre-optimizing the conventional metal insert filter ($l_1 - l_{N-1}$) [2] and the stub sections ($d_1 - d_6$) separately. An optimization routine based on the evolution strategy [9] finally fine-tunes the complete structure according to specified characteristics.

III. RESULTS

Figs. 3a and 3b show the different frequency responses of a loosely and a tight coupled Ka-band stopband section, respectively. Due to passband return losses below 10dB the loosely coupled version is not suitable for the purpose of this application. However, the reduction of the coupling length $d(d_2, d_5$ in Fig. 2b) to the order of magnitude of the strip thickness results in two attenuation peaks separated by a new passband, which is designed according to the midband frequency of the conventional metal insert filter. Both, insertion loss and return loss, can be improved by cascading two stopband sections as shown in Fig. 3c.

Fig. 4 shows the response of the new-class E-plane filter in Ka-band (solid line). The basic shape of the passband is kept constant compared with the conventional design (dashed line), whereas the skirt selectivity is increased significantly. Due to interactions of the stubs with the main filter section in certain frequency regions the stopband attenuation may be slightly lower than that of the pure metal insert filter. However, these effects only occur beyond a certain attenuation level, e.g. 50dB, which has been specified in the optimization process.

A W-band design at 94 GHz is shown in Fig. 5. Besides the improvement in stopband attenuation, special emphasis was placed on keeping the passband return loss well above the 20dB level. In fact, the VSWR increases from 1.11 (without stubs) to 1.15 (including stubs).

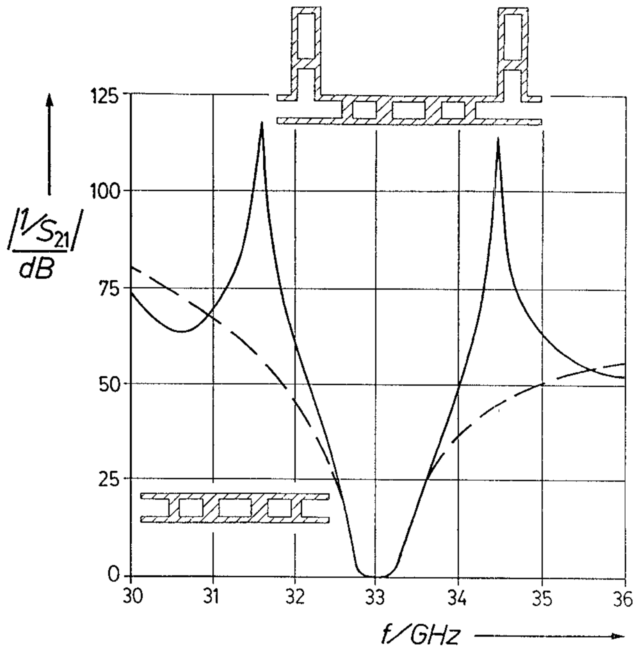

Figure 4. Insertion loss of optimized Ka-band filter: $a = 2b = 7.112$mm, $t = 0.19$mm, $d_1 = d_4 = 10.951$mm, $d_2 = d_5 = 0.2$mm, $d_3 = d_6 = 7.395$mm, $l_0 = l_8 = 8.998$mm, $l_1 = l_7 = 1.465$mm, $l_2 = l_6 = 4.286$mm, $l_3 = l_5 = 4.783$mm, $l_4 = 4.296$mm; new design (solid line), conventional metal insert filter (dashed line).

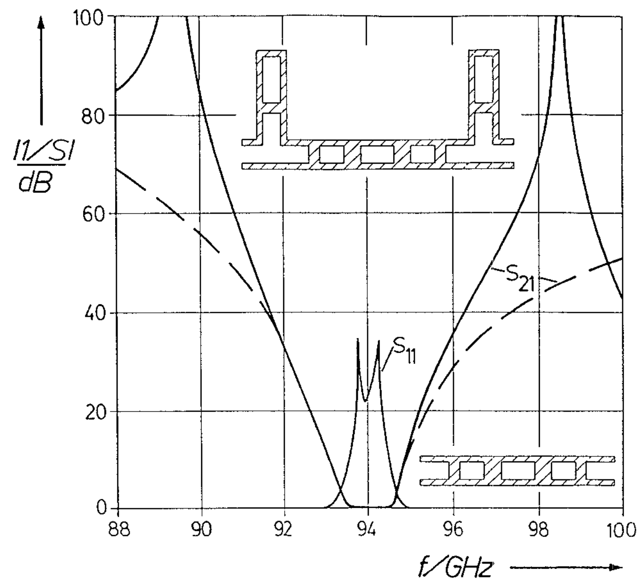

Figure 5. Return loss and insertion loss of optimized W-band filter: $a = 2b = 2.54$mm, $t = 0.05$mm, $d_1 = d_4 = 3.799$mm, $d_2 = d_5 = 0.066$mm, $d_3 = d_6 = 2.529$mm, $l_0 = l_8 = 3.495$mm, $l_1 = l_7 = 0.599$mm, $l_2 = l_6 = 1.441$mm, $l_3 = l_5 = 1.832$mm, $l_4 = 1.443$mm; new design (solid lines), conventional metal insert filter (dashed line, insertion loss only).

IV. CONCLUSIONS

A new E-plane integrated circuit filter structure has been introduced, which is capable of improving the skirt selectivity and stopband attenuation compared with conventional millimeter-wave designs. The component can easily be realized utilizing E-plane manufacturing facilities, and it is well suited for applications beyond 100 GHz. Due to a rigorous field theory treatment no tuning elements are required. The design software is PC-compatible.

REFERENCES

[1] Shih, Y.-C., "Design of waveguide E-plane filters with all-metal inserts", IEEE Trans. Microwave Theory Tech., vol. MTT-32, pp. 695-704, July 1984.

[2] Vahldieck, R., J. Bornemann, F. Arndt, and D. Grauerholz, "Optimized waveguide E-plane metal insert filters for millimeter-wave applications", IEEE Trans. Microwave Theory Tech., vol. MTT-31, pp. 65-69, Jan. 1983.

[3] Arndt, F., J. Bornemann, D. Heckmann, C. Piontek, H. Semmerow, and H. Schueler, "Modal S-matrix method for the optimum design of inductively direct-coupled cavity filters", IEE Proceedings, vol. 133, Pt. H., pp. 341-350, Oct. 1986.

[4] Bornemann, J. and F. Arndt, "Metal insert filters with improved characteristics", IEE Proceedings, vol. 133, Pt. H., pp. 103-107, Apr. 1986.

[5] Vahldieck, R. and W.J.R. Hoefer, "Finline and metal insert filters with improved passband separation and increased stopband attenuation", IEEE Trans. Microwave Theory Tech., vol. MTT-33, pp. 1333-1339, Dec. 1985.

[6] Frenna, J., "Realization of dual-mode longitudinal filters with arbitrary polarization of input and output ports", in 1986 IEEE MTT-S Digest, pp. 253-256.

[7] Zaki, A.K., C. Chen, and A.E. Atia, "A new realization of dual mode dielectric resonator filters", in Proc. 17th European Microwave Conf., pp. 169-174, Sept. 1987.

[8] Kobayashi, Y. and K. Kubo, "Canonical bandpass filters using dual-mode dielectric resonators", in 1987 IEEE MTT-S Digest, pp. 137-140.

[9] Bornemann, J., R. Vahldieck, F. Arndt, and D. Grauerholz, "Optimised low-insertion-loss millimeter-wave fin-line and metal insert filters", The Radio and Electronic Engineer, vol. 52, pp. 513-521, Nov./Dec. 1982.

[10] Matthaei, G., L. Young, and E.M.T. Jones. Microwave Filters, Impedance-matching networks, and Coupling Structures. Artech House, 1980, ch. 12.

[11] Shigesawa, H., M. Tsuji and K. Takiyama, "Two-path cutoff waveguide dielectric resonator filters", in 1985 IEEE MTT-S Digest, pp. 357-360.

[12] Arndt, F., I. Ahrens, U. Papziner, U. Wiechmann, and R. Wilkeit, "Optimized E-plane T-junction series power dividers", IEEE Trans, Microwave Theory Tech., vol. MTT-35, pp. 1052-1059, Nov. 1987.

[13] Kuehn, K., "A mode-matching method for solving field problems in waveguide and resonator circuits", Arch. Elektr. Uebertr., vol. 27, pp. 511-518, Dec. 1973.